Food Chemistry: X 25 (2025) 102218

Contents lists available at ScienceDirect

Food Chemistry: X

journal homepage: www.sciencedirect.com/journal/food-chemistry-x

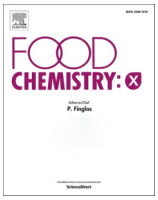

Controlling pea starch gelatinization behavior and rheological properties by modulating granule structure change with pea protein isolate

Jiwei Kuang [a,b,c], Wengang Zhang [b,c], Xijuan Yang [b,c,*], Ping Ma [d]

[a] State Key Laboratory of Plateau Ecology and Agriculture, Qinghai University, Xining, Qinghai Province 810016, China
[b] Key Laboratory of Agricultural Product Processing on Qinghai-Tibetan Plateau, College of Agricultural and Forestry Sciences, Qinghai University, Xining, Qinghai Province, 810000, China
[c] Laboratory of Qinghai-Tibetan Plateau Germplasm Resources Research and Utilization, Qinghai Academy of Agricultural and Forestry Sciences, Xining, Qinghai Province 810000, China
[d] Qinghai Tianyoude Technology Investment Management Group Co, Ltd, Xining, Qinghai Province 810016, China

ARTICLE INFO

Keywords:
Pea starch
Pea protein isolate
Starch gelatinization
Flow behavior
Granule structure

ABSTRACT

The purpose of this study was to investigate how the gelatinization behavior of pea starch (PS) was affected by pea protein isolate (PPI). The findings revealed that higher PPI levels decreased the swelling power of PS. Incorporating PPI raised the hot paste viscosity of PS, lowered the pasting temperature, and notably increased the gelatinization enthalpy according to differential scanning calorimetry analysis. Furthermore, the presence of PPI reduced the storage moduli of the starch paste, enhanced shear thinning behavior, and hindered starch molecular chain aggregation. With increasing PPI content from 0 to 12 %, amylose leaching and gel strength decreased by 25.6 % and 38.2 % respectively, indicating weak gel formation induced by PPI in PS. Confocal laser scanning microscopy confirmed that PPI envelopment of starch granules restricted their gelatinization by limiting granule swelling. These results carry significant implications for crafting pea-based foods with desired texture.

1. Introduction

Peas, being one of the most significant leguminous crops, are extensively cultivated across multiple countries and account for roughly 36 % of global legume production (Wu et al., 2023). In China, peas occupy a significant position among edible legume crops owing to their balanced and comprehensive nutritional profile. They are highly favored by consumers and represent an important source of food.

Pea seeds exhibit a carbohydrate content of 50 % - 60 %, wherein starch accounts for approximately 35 % - 40 % of the total (Farshi, Mirmohammadali, Rajpurohit, Smith, & Li, 2024). Pea starch, which is the main by-product of protein extraction is also being widely used in industry as a comparatively inexpensive source of starch compared to corn, wheat, and potato starches. However, its application in the food industry is limited due to its high extent of retrogradation and there is a need for some modification in its functional qualities to be effectively used in the food industry (Xu & Kuang, 2024a). Therefore, a comprehensive understanding of the structural and characteristic transformations of pea starch during the gelatinization process is imperative for refining the processing of pea starch-based foods.

In addition to starch, protein is a crucial component of pea seeds (Lu, He, Zhang, & Bing, 2020). Given its low cost, high protein content, absence of genetic modifications, and the fact that it is not a common allergen (unlike the eight major food allergens: milk, eggs, fish, crustacean shellfish, tree nuts, peanuts, wheat, and soybeans, which account for nearly 90 % of food allergies), it is an excellent ingredient for fortifying food products (Farshi et al., 2024). The presence of starch and protein in food matrices potentially impacts the final rheological, sensory, and other properties of the products through starch-protein interactions. Heat-induced interactions between starch and protein is complex due to the thermodynamic incompatibility among biopolymers. (Kumar, Brennan, Brennan, & Zheng, 2022). They could give rise to various types of colloidal complexes, including protein-starch complexes, protein-protein complexes, and protein aggregates embedded within starch hydrogels. The specific types of interactions played a vital role in determining the phase stability, texture, and digestibility of food matrices containing the two ingredients.

Considerable research efforts had been dedicated to investigating the

* Corresponding authors at: Key Laboratory of Agricultural Product Processing on Qinghai-Tibetan Plateau, College of Agricultural and Forestry Sciences, Qinghai University, Xining, Qinghai Province, 810000, China.
E-mail address: 2007990025@qhu.edu.cn (X. Yang).

https://doi.org/10.1016/j.fochx.2025.102218
Received 18 July 2024; Received in revised form 13 January 2025; Accepted 23 January 2025
Available online 25 January 2025

starch -protein interactions. For example, Kong, Niu, Sun, Han, and Liu (2016) demonstrated that porcine plasma protein hydrolysates could form a matrix surrounding maize starch, leading to the inhibition of starch gelatinization. Sun, Sun, and Xiong (2014) reported that the presence of peanut protein reduced the swelling power and gelatinization enthalpy of pea starch, and weakened gel strength, likely due to competition for free water absorption between protein and starch. Wu et al. (2023) also found that increasing the amount of rice protein decreased the viscosity and gelatinization temperature of rice starch while moderately enhancing gel uniformity and thickness. These observations are attributed, at least in part, to the interactions between starch and protein. Maize starch, pea starch, and rice starch possess similar crystalline structures and undergo typical gelatinization processes. However, pea starch exhibits greater sensitivity to post-gelatinization shear and forms more stable gel systems (Ratnayakea, Hoovera, & Warkentin, 2002). Hence, previous studies on the thermal and structural properties of other cereal starches might not directly apply to pea starch.

Indeed, research had indicated that pea protein could also inhibit the gelatinization of oat starch (Kumar et al., 2022). Furthermore, it had been observed that higher protein content resulted in greater fluidity in the mixed system (Pang et al., 2022). It was plausible to assume that the gelatinization process of pea starch could be limited by the presence of pea protein. However, researchers have yet to determine the critical addition level and detailed changes in the thermal properties and textural characteristics of the protein-fortified starch mixture. This knowledge gap hampers the co-application of pea starch and pea protein components in food formulation design.

Therefore, the purpose of this study was to examine how different mass fractions of pea protein isolate affected the gelatinization behavior and structural characteristics of pea starch. To accomplish this objective, the gelatinization properties, granular state, microstructure, and molecular chain morphology of pea starch were analyzed. The results of this investigation contributed to our understanding of how pea starch and protein interacted at gelation phases and how that affected starch gelatinization. The findings may be applied in formulating and processing protein-fortified nutrition formula in which the pea protein and starch interactions and coacervations determine phase stability and textural nature of processed foods.

2. Materials and methods

2.1. Materials

Pea starch (PS, purity >98 %) and pea protein isolate (PPI, purity ≥80 %) were purchased from Shanghai Yuanye Biotechnology Co., Ltd. in China. All other chemical reagents used were of analytical reagent grade.

2.2. Preparation of samples

To systematically investigate the influence of PPI quality on the gelatinization behavior of PS, a single-factor experimental design was implemented, wherein varying quantities of PPI were incorporated into a fixed mass of PS. Specifically, 10 g of PS was blended with PPI at concentrations of 3 %, 6 %, 9 %, and 12 % based on the weight of the starch. The resultant mixtures were designated as +3 %PPI, +6 %PPI, +9 %PPI, and + 12 %PPI, respectively, to facilitate clear identification and analysis. For comparison, a control group consisting only of PS without PPI was included.

2.3. Determination of swelling power

The swelling power was determined according to the method described by Kong et al. (2016). PPI at concentrations of 0 %, 3 %, 6 %, 9 %, and 12 % based on the dry weight of the starch were added to the dispersion of 2 % (*w/v*) PS. The aqueous PS/PPI slurry was heated with stirring at 65 °C, 75 °C, 85 °C, and 95 °C for 30 min. Subsequently, the sample was rapidly cooled to room temperature using an ice water bath. After centrifugation at 4000 ×*g* for 15 min at 20 °C, the precipitate was weighed (Mp) and dried at 105 °C until a constant weight (Md). The swelling power was calculated by dividing the weight of the precipitate by the weight of dry starch, and the results were expressed as Mp per Md (g/g).

2.4. Pasting property measurement

The viscosity profiles of starch pasting in an aqueous system were measured using a rapid viscosity analyzer (RVA-TM, Perten Instruments Ltd., Sweden) following the method described by Hou et al. (2020). A total of 2.8 g of dry PS, containing various ratios of PPI, was mixed with deionized water to achieve a total dispersion weight of 28 g. The samples were first premixed using a paddle stirrer at 960 rpm for 10 s, followed by stirring at 160 rpm for 50 s at 50 °C. Subsequently, the samples underwent a controlled heating and cooling process: heating from 50 °C to 95 °C at a rate of 12 °C/min, holding at 95 °C for 2.5 min, cooling back to 50 °C at a rate of 12 °C/min, and finally maintaining the temperature at 50 °C for an additional 2 min. During the tests, data such as pasting temperature, peak viscosity, trough viscosity, final viscosity, breakdown viscosity, and setback viscosity were recorded.

2.5. Determination of differential scanning calorimeter (DSC)

DSC (Q2000, TA Instrument, New Castle, DE, USA) was employed to determine the thermal properties of PS and its mixtures with PPI by the modified method of Kuang, Ma, Pu, Huang, and Xiong (2021). Technical support for the analysis was provided by Sanshu Biotech Co., LTD. Initially, approximately 3 mg of the sample was placed onto an aluminum pan and then hydrated with deionized water at a ratio of 1:3 (*w*/w, sample/water). Subsequently, the sealed pans were balanced at 25 °C for a duration of 24 h, and then heated from 25 °C to 100 °C at a constant rate of 10 °C/min. An empty pan was used as a reference during the analysis. From the DSC curve, several parameters include the the denaturation onset temperature (T_o), peak temperature (T_p) and conclude temperature (T_c), and gelatinization enthalpy (ΔH) were determined.

2.6. Rheological measurement

The rheological properties of PS and its mixture with PPI were assessed using a Haake-Mars 60 rheometer (Thermo Scientific, Karlsruhe, Ger-many) equipped with a parallel plate measuring 35 mm in diameter and 0.5 mm in gap (Ji et al., 2023). In a 6 % (*w/v*) PS suspension, various proportions of PPI (0, 3 %, 6 %, 9 %, and 12 %, based on the mass of PS) were added and magnetically stirred at 25 °C for 30 min. PS slurry containing different proportions of PPI was applied onto the fixture. The following rheological tests were then initiated:

(1) Temperature sweep test. The suspension was balanced at 50 °C for 5 min, and then heated from 40 °C to 95 °C at a rate of 5 °C/min. The strain was set to 0.5 % and the frequency to 1 Hz. Storage modulus (G′) against time (s) was recorded.
(2) Stable flow test. After completing the measurements in step (1), the samples were cooled to 25 °C for stable flow measurement. Specifically, after equilibrating at 25 °C for 5 min, measurements were taken at a shear rate ranging from 0.1 to 100 s^{-1} at a constant strain.

2.7. Determination of leached amylose

The content of leached amylose was quantitatively analyzed using iodine colorimetric reaction (Zhou et al., 2014). Following the method

described in Section 2.4, PS suspensions (5 %, *w/v*) containing various masses of PPI underwent a pasting treatment. The PS-PPI pastes prepared above were then transferred into 50 mL centrifuge tube, centrifuged at 15000 *g* for 20 min and collected the supernatant. Then, 1 mL of the supernatant was dissolved in 6 mL of 0.33 mol/L NaOH solution, mixed thoroughly, and heated at 95 °C for 30 min. The pH of the solution was adjusted to 5.5 using 0.5 % trichloroacetic acid, followed by the addition of 0.05 mL of 0.01 mol/L I_2-KI solution. After incubating at room temperature for 30 min, the absorbance of the solution was measured at 620 nm.

2.8. Fourier transform infrared spectroscopy (FTIR) analysis

Secondary structures of PPI were determined utilizing an FTIR spectrometer (Vertex 70, Bruker, Germany) according to the method described by Xu and Kuang (2024b). The samples were prepared by mixing them with solid KBr powder at a weight ratio of 1:60, followed by compressed into a slice. Spectral data was collected with 64 scans at a resolution of 4 cm^{-1} across the wavenumber range of 400–4000 cm^{-1}. The obtained spectra were processed using OPUS 7.2 software for baseline correction and normalization. The secondary structure was determined from the amide I region (1600–1700 cm^{-1}) through Fourier self-deconvolution (FSD) and curve fitting. The assignments for secondary structural elements were as follows: β-sheet (1600–1640 cm^{-1} and 1681 cm^{-1}), random coil (1640–1650 cm^{-1}), α-helix (1650–1660 cm^{-1}), and β-turn (1660–1670 cm^{-1} and 1694 cm^{-1}).

2.9. Gel strength measurement

The PS-PPI paste prepared in section 2.4 was transferred into a 25 cm × 40 cm (length × diameter) cylindrical mold. In detail, the mold was filled with equal portions of the starch paste and then cooled to room temperature to allow the formation of a set gel. A TA-XT Plus texture analyzer (Stable Micro Systems Ltd., Surry, UK) equipped with a P/0.5 plane cylindrical probe was used to determine the strength of the gel. The gel penetration test was conducted with the following parameters: a pre-test speed of 5 mm/s, a test speed of 1 mm/s, a post-test speed of 5 mm/s, and a sample deformation of 8 mm (Kuang et al., 2021). The strength of the gel was defined as the initial pressure in Newtons (N) required to puncture the gel during the test.

2.10. Atomic force microscopy (AFM) observation

The molecular chain morphology of the sample was observed using a Nanoscope MM8 type AFM in ScanAsyst mode, equipped with ScanAsyst-Air probes (Bruker Co., Santa Barbara, CA), following the method described by Kuang et al. (2022). For the preparation of AFM samples, 0.1 g of PPI powder, PS particles, and PS-PPI blends were each separately mixed with 10 mL of deionized water. The mixture was heated in a 90 °C water bath for 15 min. After cooling to room temperature, the sample concentration was diluted to 0.1 mg/mL with deionized water. Subsequently, 5 μL of the diluted sample was spread onto a freshly cleaved mica sheet (Φ ≈ 15 mm) (Tosai Co., Japan). The sample on the mica sheet was *v*acuum dried for 3 h before scanning. The scanning of the AFM samples was performed in a light tapping mode with a scanning area of 5 μm × 5 μm. The AFM probe used had a spring constant of 0.4 N/m and a resonant frequency of 1 Hz. The obtained AFM images were analyzed using NanoScope *v*ersion 1.18 software (Bruker Co., Santa Barbara, CA). The root mean square roughness, average molecular chain height and width were determined from the analyzed AFM images.

2.11. Confocal laser scanning microscopy (CLSM) observation

CLSM was applied to investigate the distribution pattern of PPI around the surface of starch granules as described by Qiu et al. (2016). The samples were prepared as section 2.7 described. Subsequently, the prepared sample were stained with the mixed solution containing fluorescein 5-isothiocyanate (FITC, 0.02 % *w/v*, preferentially labeled starch) and Rhodamine B (0.025 % w/v, preferentially labeled protein). Finally, the stained sample was evenly loaded onto a glass slide and examined for its morphology within 15 min. The excitation and emission wavelengths for FITC were set to 488/518 nm, whereas for Rhodamine B, they were set to 568/625 nm.

2.12. Statistical analysis

All data was analyzed using the SPSS 19.0 software program (SPSS Inc. Chicago, IL), and presented as the mean ± standard deviation (SD). All the experiments were performed in triplicate, unless otherwise indicated. Significant differences between the results were determined using Analysis of variance (ANOVA), and mean values were separated using Duncan's test with a confidence level of 0.95 ($P < 0.05$).

3. Results and discussion

3.1. Swelling power

As depicted in Fig. 1 A, the swelling power of pea starch (PS) exhibited a gradual increase with rising temperature. However, the inclusion of pea protein isolate (PPI) significantly reduced the swelling power of PS across various temperatures ($P < 0.05$). These results clearly indicated that the inhibitory effect of PPI on the swelling of starch granules. Generally, the swelling behavior of starch is predominantly influenced by amylopectin, whereas amylose act as an inhibitor and maintained the integrity of swollen granules to some extent (Hu et al., 2020). At the same temperature, the swelling power of PS progressively diminished with increasing amounts of PPI. This phenomenon could be attributed to the strong interactions between PPI and the amylose fractions, consequently exerting a more pronounced effect on restricting starch gelatinization. A similar trend was observed in a study by Kong et al. (2016), it was observed that the reduction in swelling power of corn starch (CS) was mainly ascribed to the combination of porcine plasma protein hydrolysates (PPPH) and starch granules, which served to stabilize the granular structure.

Additionally, the decrease in swelling power might also be associated with the physical adsorption behavior of PPI. Specifically, PPI was adsorbed onto the surface of starch granules, forming a film with a certain rigidity that prevented the leaching of some starch components and hindered the deformability of the granules (Zhou et al., 2014). The relevant reasons for these observations would be further elucidated in subsequent RVA, CLMS, and AFM analyses.

3.2. Pasting properties

The impact of PPI on the pasting behavior of PS, as measured by RVA, is shown in Fig. 1 B. It was evident that both PS and its blends with PPI exhibited similar pasting patterns. Initially, they had peak viscosity during the heating phase, followed by viscosity reduction at a temperature of 95 °C, and finally set back upon cooling (Wang et al., 2017).

The pasting parameters for each sample are presented in Table 1. The presence of PPI induced a significant decrease in the pasting temperature of PS, and this effect became more pronounced with increasing concentrations of PPI ($P < 0.05$), as evidenced by the leftward shift in the RVA curve. For example, the pasting temperature decreased significantly from 73.7 °C for native PS to 68.6 °C for PS + 12 % PPI mixtures. The gelatinization temperature obtained from RVA is associated with the initial viscosity of starch gelatinization, which in turn depends on the media viscosity (Kuang, Huang, et al., 2022). During the heating process, the gradually gelling PPI created a certain degree of steric hindrance, which inhibited the movement of starch granules during gelatinization and restricted the transfer of heat. This effect ultimately

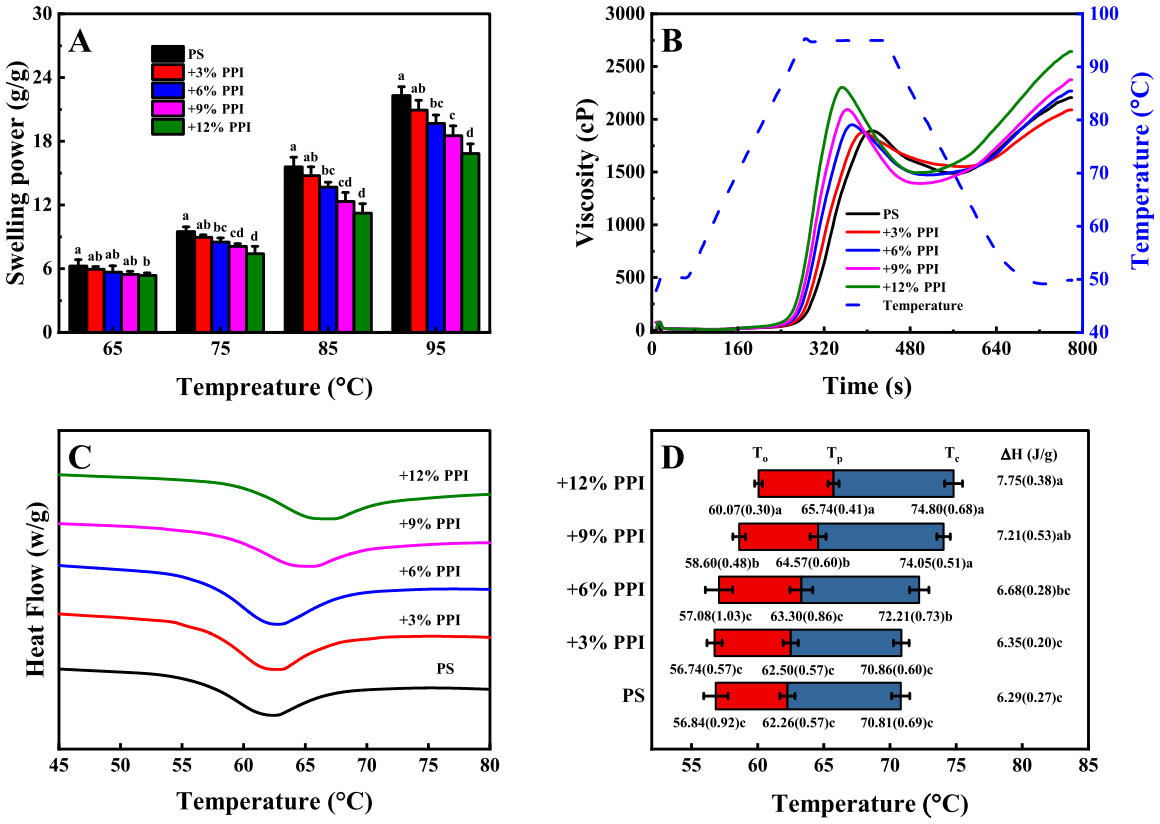

Fig. 1. Swelling power (A), pasting profiles (B), DSC curves (C), schematic overview of the gelatinization temperature ranges and enthalpic transition data (ΔH) (D) of pea starch (PS) - pea protein isolate (PPI) mixtures at different protein concentrations. Different lowercase letters of the same parameter indicate significant difference ($P < 0.05$).

Table 1
Pasting properties of pea starch (PS) - pea protein isolate (PPI) mixtures at different protein concentrations.

Samples	Pasting temperature (°C)	Viscosity (cP)				
		Peak viscosity	Trough viscosity	Final viscosity	Breakdown viscosity	Setback viscosity
PS	73.7 ± 0.1a	1899.3 ± 6.7c	1481.0 ± 6.1ab	2205.7 ± 29.1c	418.3 ± 4.2 cd	724.7 ± 24.2c
+3 % PPI	72.3 ± 0.5b	1861.3 ± 38.0c	1531.3 ± 40.3a	2101.0 ± 38.7d	363.3 ± 58.7d	603.0 ± 75.3d
+6 % PPI	70.9 ± 0.4c	1917.0 ± 32.0c	1456.0 ± 16.0b	2242.5 ± 24.5c	461.0 ± 16.0c	786.5 ± 8.5c
+9 % PPI	69.6 ± 0.1d	2024.0 ± 88.2b	1373.0 ± 25.5c	2338.0 ± 38.0b	651.0 ± 25.5b	965.0 ± 15.6b
+12 % PPI	68.6 ± 0.5e	2235.7 ± 65.0a	1452.0 ± 43.9b	2551.0 ± 85.2a	783.0 ± 43.9a	1098.3 ± 43.4a

Values are given as the means ± SD from triplicate determinations; a-e means in the same column with different letters indicate significant differences ($P < 0.05$).

led to an increase in the gelatinization temperature of PS.

The addition of PPI significantly increased the viscosity of the mixed system compared to the control, and the effect was dose-dependent. In addition to the trough viscosity, the peak viscosity, final viscosity, breakdown viscosity, and setback viscosity of the PS-PPI mixtures increased by 17.7 %, 15.7 %, 87.2 %, and 51.6 % with the PPI addition increased from 0 to 12 %, respectively. Viscosity enhancement in starch-protein mixtures was usually attributed to the swelling and deformability of starch granules during gelatinization, as well as the enhanced starch-proteins interactions in the continuous phase during heating (Zhang et al., 2021). On the one hand, the increase of the effective starch concentration in the continuous phase as a result of starch-protein interactions could lead to the detection of pasting at lower temperatures and changes in viscosity of the heated starch suspension, based on the thermodynamic incompatibility between PS and PPI (Qiu et al., 2015; Ribotta, Colombo, & Rosell, 2012). The physicochemical properties of PPI dictate that it could rapidly absorb water. Upon heating, a quickly formed semisolid network, mainly composed of highly hygroscopic PPI, formed a viscous water layer at the surface of starches (Kuang et al., 2021). This viscous water layer contributed to high viscosity. On the other hand, the observed increase in viscosity was likely attributable to the formation of heat-induced PPI aggregates. Specifically, during the denaturation process, the free thiols in PPI were shown to react with thiol groups in other protein molecular chains, resulting in the formation of dimers, trimers, and tetramers. At low concentrations, these aggregates remained relatively small and exerted a minor influence on the overall viscosity. However, at critical concentrations of PPI, they could form a three-dimensional gel network, significantly contributing to the system's viscosity (Fig. S1) (Kumar et al., 2022; Wu, Gong, et al., 2023).

This significant increase in viscosity could be explained using the theory of van der Waals equation of state and the free volume concept (van der Sman, 2012). For simplicity, the swollen starch granules and protein aggregates could be considered as hard spheres. The addition of PPI solids and the subsequent formation of protein aggregates reduced the free volume and free energy of the aqueous phase within the starch dispersion. In such a concentrated dispersion system, particle mobility became restricted, leading to the formation of a soft-glass structure with a degree of percolation, which consequently resulted in a significant

increase in viscosity. To summarize, PPI affected the pasting behavior of PS, which was due to its water-holding capacity and reduced free volume of the starch dispersion system. The other reasons could be attributed to the formation of PPI aggregates, which could interact with starch molecules and to the transition from unjammed state to jammed state.

3.3. Thermal properties

The DSC curves of all samples exhibited a similar pattern in Fig. 1 C, with a distinct endothermic peak observed within the range of 60–65 °C, indicative of starch gelatinization. According to the results calculated from the DSC curves, the onset temperature (T_o), peak temperature (T_p) and conclude temperature (T_c) are presented in Fig. 1 D. As the amount of PPI increased, the values of T_o, T_c, T_p, and ΔH displayed a gradual increase. For instance, T_o, T_p, and Tc significantly increased from 56.84 °C, 62.26 °C and 70.81 °C for natural PS to 60.07 °C, 65.74 °C, and 74.80 °C for PS + 12 % PPI mixtures, respectively. The transition temperatures became higher for starch suspensions when PPI was added. This effect could be attributed to two potential explanations. Firstly, the increasing amount of PPI resulted in a significant reduction in the availability of "free water" in the starch suspension, necessitating higher transition temperatures to overcome the challenges posed by water scarcity during starch gelatinization (Kuang et al., 2021). Secondly, it was possible that the PPI chains encapsulated the starch granules during the heating process, thereby limiting the amount of water absorbed by the particles (Wang, Ye, et al., 2017). Consequently, the gelatinization of PS occurred at elevated temperatures as the PPI content increased.

In addition, as the PPI content in the PS-PPI mixtures increased, the gelatinization enthalpy (ΔH) exhibited a corresponding upward trend. For instance, the gelatinization enthalpy rose from 6.29 J/g to 7.75 J/g As the PPI content increased from 0 to 12 %. These findings were basically consistent with those reported by Kuang, Huang, et al. (2022), they found that this phenomenon was attributed to the enhanced interactions between PPI and PS, resulting in the stabilization of the molecular structure of starch chains, particularly within the crystalline region. Wang, Zheng, Yu, Wang, and Copeland (2017) also proposed that β-lactoglobulin could impede interactions among starch chains during DSC heating by inserting into the amylose helix. Likewise, PPI with low molecular weight may also integrate into the helical structure of amylose, thereby manifesting their role in maintaining the structural integrity of the starch granules. The inhibitory effects of PPI on the crystalline melting of PS lead to a reduced extent of conformational disordering of the molecular chains during heating (Kong et al., 2016; Yang, Zhong, Goff, & Li, 2019). This implied that higher thermal energy input was required to disrupt the molecular structure of starch chains during gelatinization, resulting in an increase in ΔH. This observation was consistent with the results of RVA measurement.

3.4. Rheological properties

3.4.1. Temperature sweep

The time-dependent changes in storage moduli (G') during the heating and holding stages are presented in Fig. 2 A. The influence of PPI on the elasticity of the system varied depending on the heating conditions. During the initial heating stage (50–95 °C), G' exhibited a sharp increase around 66 °C and reached its peak at 95 °C, primarily due to the gelatinization of starch granules. This process involved the rapid swelling of starch granules and the subsequent leaching and dissolution of amylose (Yang et al., 2019). The amylose molecules were able to form a stable three-dimensional network structure by interacting with the external amylopectin, resulting in an increase in G'. During the subsequent holding stage at 95 °C, G' rapidly decreased. This phenomenon could be attributed to the increased mobility of amylose at high temperature, leading to the weakening or even breaking of hydrogen bonds within the gel network structure (Zhu, Bertoft, & Li, 2016).

Notably, the addition of PPI substantially reduced the G' of starch during heating, and this effect was dependent on the concentration of PPI. The strength of the starch gel was found to be influenced not only by the content of leached amylose but also by the structure of swollen starch granules (Hou et al., 2020). The decrease in G' induced by PPI could be attributed to multiple factors. These included the inhibition of PPI on amylose leaching, the inhibition on starch particle expansion, and the disruption of hydrogen bond formation among the starch molecules (Yang et al., 2019). These combined effects ultimately led to a reduction in G'.

3.4.2. Flow behavior

As observed in Fig. 2 B, the shear stress of all samples exhibited an increase with an increase in shear rate. This result indicated the manifestation of non-Newtonian flow characteristics, which was a typical behavior of many polysaccharides in water dispersion (Chen, Zhang, Li, Xie, & Chen, 2018). The impacts of PPI on the shear stress of PS depended on the concentration added. Specifically, an increase in PPI content resulted in a gradual decreased in the shear stress of starch pastes, suggesting that the network structure of PS-PPI mixtures offered less resistance to shear conditions.

PPI were mainly composed of low molecular weight water-soluble albumin and salt-soluble globulin (Boukid, Rosell, & Castellari, 2021; Lam, Karaca, Tyler, & Nickerson, 2018). During heating, the molecular chains of PPI gradually unfolded and maintained an extended form, enabling easier interactions with amylose molecules. Consequently, the formation of the starch gel network was inhibited, leading to an increased level of pseudoplasticity in the starch paste (Kuang et al., 2021). At higher shear rates, the dynamic network formed by the intertwining of amylose molecules and PPI molecular chains in the junction region became highly unstable and susceptible to disruption,

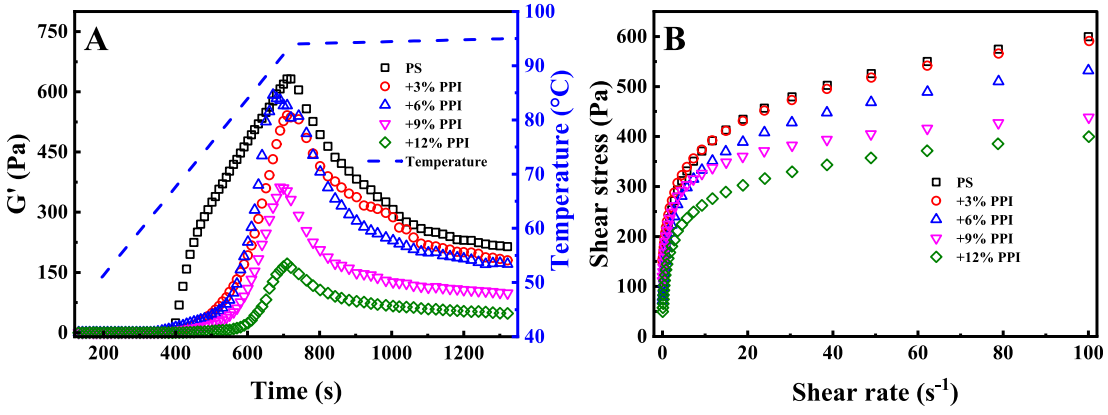

Fig. 2. Temperature sweep (A) and steady shear flow curves (B) of pea starch (PS) - pea protein isolate (PPI) mixtures at different protein concentrations.

resulting in more pronounced shear thinning.

3.5. Leaching of amylose

As shown in Fig. 3 A, the amylose leaching amount of PS-PPI mixture was significantly lower than that of PS alone ($P < 0.05$). With an increase in PPI content from 0 to 12 %, the leaching of amylose decreased by 25.6 %. This reduction could be attributed to the increased viscosity of the continuous phase, which hindered the diffusion of amylose from the starch granules, consistent with findings by Zheng et al. (Zheng et al., 2019). The extent of amylose leaching outside the granules generally depends on the granule swelling and the molecular structure of amylose during starch gelatinization (Kuang et al., 2021). On the one hand, the formation of a high-viscosity PPI network structure upon heating allowed for its adsorption onto the starch granules, forming a dense film with certain rigidity that inhibited amylose leaching (Qiu et al., 2015; Zhou et al., 2014). This was supported by the experimental results of swelling power, indicating that the increased PPI content significantly impeded granule swelling and rupture, consequently reducing amylose leaching outside the granules.

On the other hand, the formation of stable complexes through intermolecular hydrogen bonds or chain entanglements between amylose molecules and PPI molecules could contribute to the reduction in detectable amylose in the system (Kett et al., 2013; Kong et al., 2016). As reported by Kuang et al. (2021), they found that the low molecular weight proteins could penetrate into the swollen starch granules and form a restrictive network with amylose molecules, preventing the leaching of certain amylose fractions from the granules.

To further elucidate the observed reduction in amylose leaching, the modifications in the secondary structure of PPI were analyzed using infrared spectroscopy. The FTIR spectra of PPI are shown in Fig. S2 A, revealing consistent trends across all samples. To quantify the changes in the secondary structure of PPI, the relative percentages of secondary structural components for each sample are presented in Fig. S2 B. Notably, β-sheet constituted the predominant secondary structure in raw PPI powder, with its proportion exhibiting a progressive increase during the formation of heat-induced gels. The contents of α-helix and β-sheet significantly decreased in PS + PPI mixtures compared to PPI gel, while the proportions of random coil and β-turn gradually increased. Generally, β-sheet is indicative of the degree of protein molecular aggregation, with a higher β-sheet content corresponding to a more stable gel structure (Kuang et al., 2022). In PS - PPI mixtures, the marked reduction in β-sheet content facilitated the formation of lower-energy structural arrangements composed primarily of β-turns and random coils, which were less conducive to the stabilization of protein networks. This structural transition was likely attributable to interactions between amylose and PPI molecular chains. Similarly, Xu and Kuang (2024b) reported analogous findings, suggesting that the interaction between short-chain starch molecules and gluten protein chains was a primary factor contributing to the reduced structural stability of gluten proteins, ultimately leading to protein depolymerization and morphological changes.

3.6. Penetration testing

Penetration testing proved to be a valuable method for assessing the strength of starch gel, as it reflects the degree of cross-linking among starch molecules. Fig. 3 B demonstrated that the native PS gel had a penetration force of 2.58 N, which was significantly reduced upon the addition of PPI ($P < 0.05$). Specifically, increasing the PPI content from 0 to 12 % resulted in a 38.2 % reduction in penetration force. The decrease in PS gel strength caused by PPI could be primarily attributed to the reduction in amylose leaching during heating. As the PPI content increased, the leaching of amylose gradually decreased, establishing it as the main reason for the reduced gel strength (Kong et al., 2016). This correlation between gel strength decreases and amylose leaching reduction aligned with the findings mentioned earlier.

Furthermore, Cui, Fang, Zhou, and Yang (2014) reported that the decline in starch gel strength was not solely dependent on the amylose leaching content but also related to the weak network structure formed by the interaction between starch and protein molecules. This starch-protein combinations could hinder the formation of hydrogen bonds among starch chains, thereby resulting in the “weak gel” characteristic of PS-PPI mixtures.

3.7. AFM

Atomic Force Microscopy (AFM) was applied to investigate the impact of PPI on the nanostructure morphology of PS. As shown in Fig. 4, the deposition of PPI on the mica substrate revealed an aggregation structure which was characterized by the bright regions observed in the AFM 2D image. These bright spots were speculated to arise from the aggregation of multiple PPI chains or the folding of individual PPI chains within the cross-section (Liang et al., 2022). Comparison with PPI alone, it was observed that the gelatinized PS exhibited significantly larger molecular chain sizes and displayed a dense network structure. As the concentration of PPI increased, the PPI molecules tightly bound to the surface of PS molecules and hindered the cross-linking among the molecular chains of PS, which decreased the aggregation degree among PS molecular chains. This behavior was attributed to the self-aggregation tendencies exhibited by PPI molecular chains under heating.

The AFM 3D images depicted PPI molecular chains in the rod-like conformations on a nanometer scale (Fig. 5 A), with the root mean

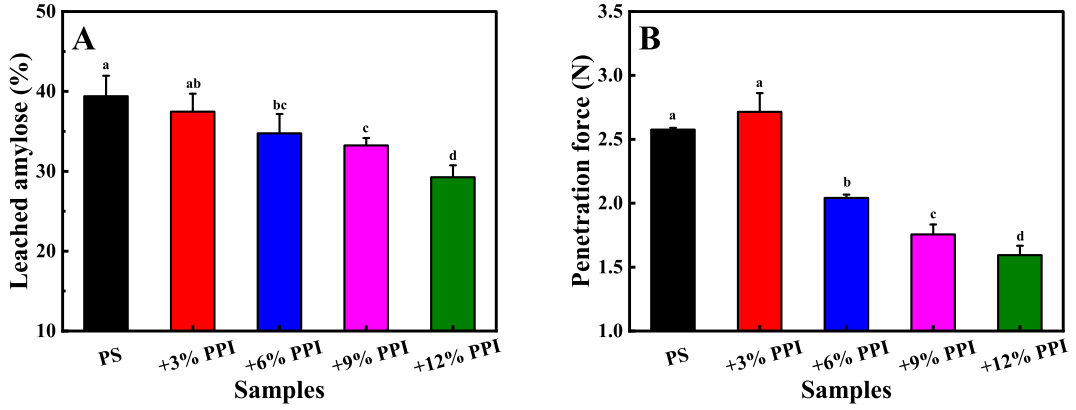

Fig. 3. The amount of amylose leached from the starch granules (A), penetration force (B) of pea starch (PS) - pea protein isolate (PPI) mixtures at different protein concentrations.

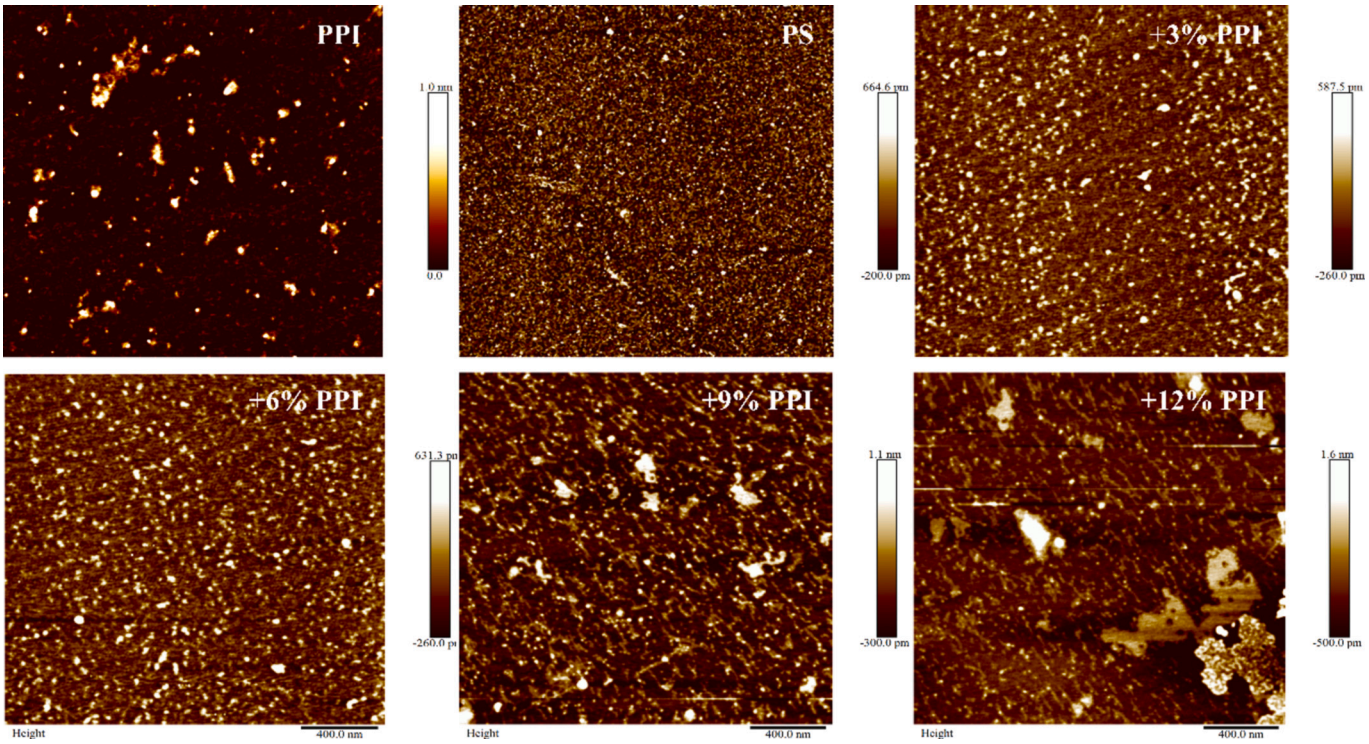

Fig. 4. The 2D images of AFM morphology of individual pea protein isolate (PPI), and pea starch (PS) - pea protein isolate (PPI) mixtures at different protein concentrations.

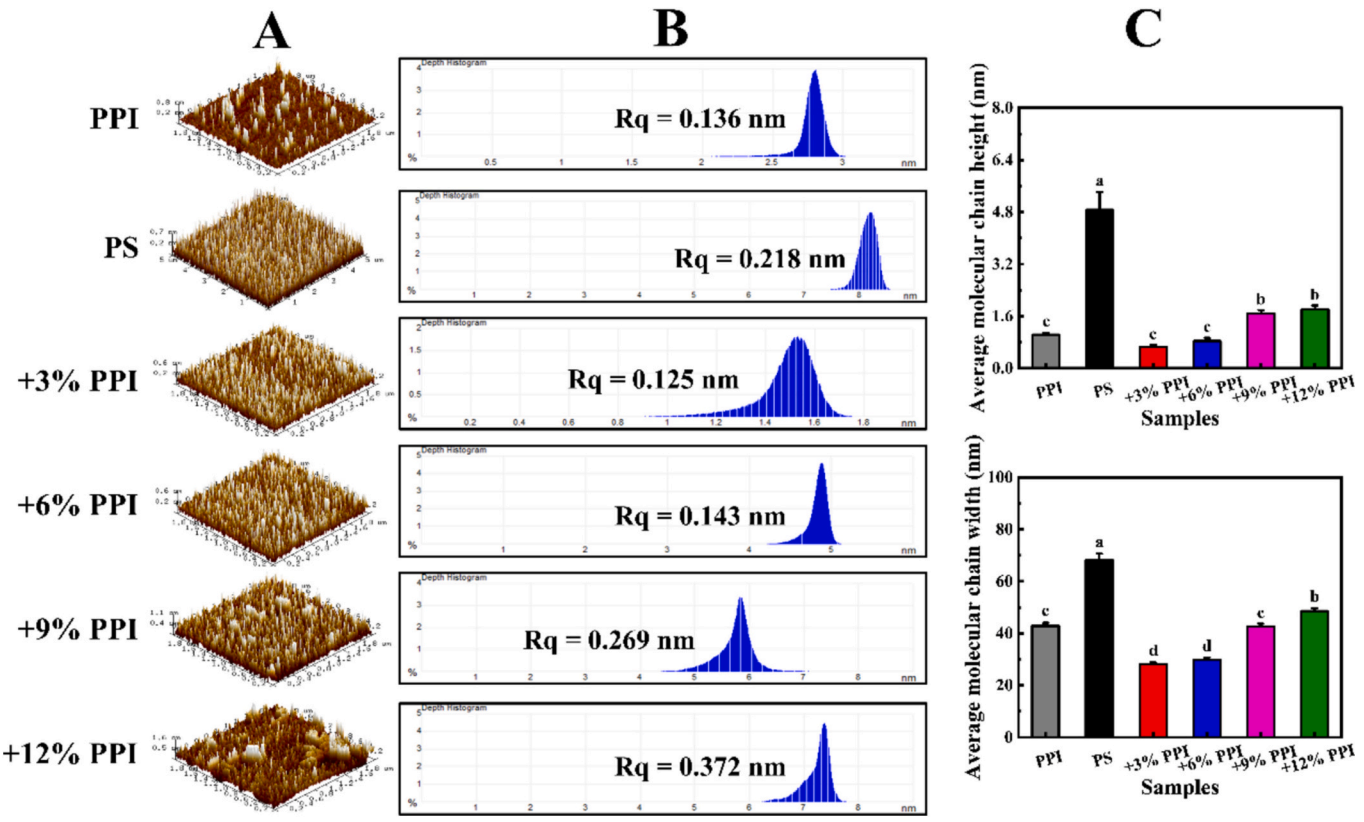

Fig. 5. The 3D images of AFM morphology (A), depth histogram (B), average molecular chain height/width (C) of individual pea protein isolate (PPI), and pea starch (PS) - pea protein isolate (PPI) mixtures at different protein concentrations.

square roughness (Rq) of 0.136 nm (Fig. 5 B) and the average molecular chain height/width of 1.03/42.8 nm (Fig. 5 C). These dimensions were consistent with the reported size of peptide aggregates in aqueous solutions by Niu, Wu, and Xiao (2017). The molecular chains of PS appeared as thinner linear structures with a larger Rq and the average molecular chain height/width than that of PPI. This difference might be a manifestation in different aggregation degrees of macromolecular chains (An, Yang, Liu, & Zhang, 2008; Tang & Copeland, 2007).

Compared with the PS alone, it was observed that the bright regions in the mixtures become more pronounced, but the changes of molecular size were greater. Specifically, upon the addition of 12 % PPI, the Rq of the mixtures were measured as 0.372 nm, which indicated that PPI significantly interfered with the aggregation of starch molecular chains. Interestingly, as the PPI content increased, the height and width of the molecular chains in the mixtures gradually increased but remained smaller compared to those of PS. These results could be attributed to the self-aggregation effect of PPI under thermal induction. As the content of PPI increased, the interaction between the protein molecular chains significantly enhanced, and the aggregation phenomenon became more pronounced. Ultimately, this resulted in brighter areas being formed in the AFM images (Liang et al., 2022; Wu, Gong, et al., 2023). These interactions might contribute to the slightly increased molecular chain size in the mixtures with higher protein content.

3.8. CLSM

The microstructure of the gelatinized starch and its mixture with PPI were observed by CLSM (Fig. 6). In the CLSM micrograph, starch and protein were labeled in green and red, respectively. For PS alone, the starch granules appeared damaged and disrupted, with the presence of starch residues blurring the boundaries of the granules. This was consistent with the findings described by Zhou et al. (2014) regarding the gelatinization behavior of wheat starch, wherein under the influence of high temperatures, starch granules were compromised and eventually ruptured. Consequently, starch components diffused outward from the granules, forming a continuous and glutinous network around the surface of the swollen granules. In contrast, when PPI was present, the starch granules appeared smaller and the granule morphology became clearer. This observation indicated that PPI played a role in retaining the swollen size and structure of the starch granules, possibly by restricting starch granule swelling (Kuang et al., 2021), as consistent with the results obtained from swelling power determination.

As the content of PPI increased, it was found that PPI was more prominently distributed in the peripheral layer of the swollen starch and acted as a protective or lubricating “barrier”, stabilizing the granule structure (Qiu, Yadav, et al., 2015). This mechanism was similar to the effect of hydrocolloids on starch granules during the gelatinization process (Chaisawang & Suphantharika, 2005; Heyman, Depypere, Meeren, & Dewettinck, 2013). Specifically, the hypothetical mechanism of interactions between PS and PPI during heat treatment might be explained as follows: PPI formed self-assemblies, and then both unfolded PPI and PPI aggregates were adsorbed onto the starch granules, forming a protein film or shell at the exterior of PS granules. As a result, this protein film acted as a barrier for water migration from the bulk aqueous phase to the starch granules, thereby reducing the leaching of amylose and the swelling of starch granules. Furthermore, it was also observed that PPI could penetrate into the swollen starch granules and bind to some starch components. During the heating process, the surface of the granule would develop pores, allowing low molecular weight PPI to penetrate inside the swollen starch granules. Inside, it would interact with amylose molecules, thereby inhibiting the gelatinization behavior of starch through modulation of the granule structure (Kong et al., 2016).

4. Conclusions

This study demonstrated that PPI had a significant impact on the gelatinization, rheological, and structural properties of PS. The presence of PPI reduced the swelling power of PS, and more amylose remains trapped within the starch granules. Meanwhile, increasing the content of PPI decreased the pasting temperature and gelatinization enthalpy of PS, which implied that the presence of protein hampered the gelatinization process by lowering the thermal stability of the starch. Rheological analyses revealed that the flowability of starch paste was enhanced by PPI, leading to a weaker gel strength. This weakening effect could be attributed to the inhibition of starch molecular chain crosslinking by

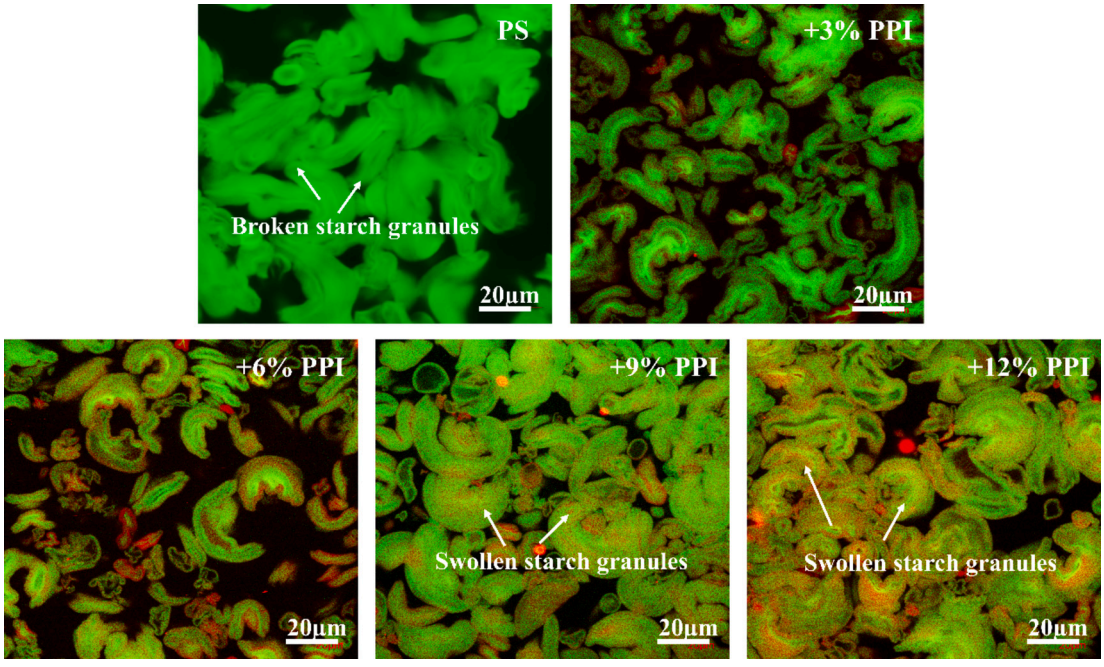

Fig. 6. CLSM images of pea starch (PS) - pea protein isolate (PPI) mixtures at different protein concentrations. Green and red in the figures correspond to starch and proteins, respectively. (For interpretation of the references to colour in this figure legend, the reader is referred to the web version of this article.)

PPI. AFM observations supported these findings by showing that PPI reduced the aggregation of PS molecular chains, which was likely due to the replacement of starch-starch interactions with protein-starch interactions caused by the addition of excessive protein. CLSM images further demonstrated that the wrapping structure of PPI provided protection to the structure of starch granules, preventing their swelling and rupture, which aligned with the observed decrease in swelling power. Overall, these results are useful to manufacturers who seek to improve food texture by using starch and protein as co-texturizers, and to develop protein-fortified cereal-based foods including bakery products, breakfast foods, dairy drinks, and ready-to-eat or ready-to-drink products.

CRediT authorship contribution statement

Jiwei Kuang: Writing – original draft, Supervision, Resources, Investigation, Funding acquisition. **Wengang Zhang:** Formal analysis, Data curation. **Xijuan Yang:** Writing – review & editing, Investigation, Funding acquisition. **Ping Ma:** Resources, Investigation.

Declaration of competing interest

The authors declare that they have no known competing financial interests or personal relationships that could have appeared to influence the work reported in this paper.

Acknowledgements

This work is supported by The Open Project of State Key Laboratory of Plateau Ecology and Agriculture, Qinghai University (2024-ZZ-04), Special Project for the Development of Innovation Platforms by the Qinghai Provincial Department of Science and Technology (2022-ZJ-T04), and Innovation Platform Construction Special Project "Laboratory of Qinghai-Tibetan Plateau Germplasm Resources Research and Utilization" (2024). The authors extend their gratitude to Ms. Zhang Yuyao from Shiyanjia Lab (www.shiyanjia.com) for providing invaluable assistance with the CLSM analysis.

Appendix A. Supplementary data

Supplementary data to this article can be found online at https://doi.org/10.1016/j.fochx.2025.102218.

Data availability

Data will be made available on request.

References

An, H., Yang, H., Liu, Z., & Zhang, Z. (2008). Effects of heating modes and sources on nanostructure of gelatinized starch molecules using atomic force microscopy. *LWT-Food Science and Technology, 41*, 1466–1471. https://doi.org/10.1016/j.lwt.2007.08.026

Boukid, F., Rosell, C. M., & Castellari, M. (2021). Pea protein ingredients: A mainstream ingredient to (re)formulate innovative foods and beverages. *Trends in Food Science & Technology, 110*, 729–742. https://doi.org/10.1016/j.tifs.2021.02.040

Chaisawang, M., & Suphantharika, M. (2005). Effects of guar gum and xanthan gum additions on physical and rheological properties of cationic tapioca starch. *Carbohydrate Polymers, 61*(3), 288–295. https://doi.org/10.1016/j.carbpol.2005.04.002

Chen, B., Zhang, B., Li, M. N., Xie, Y., & Chen, H. Q. (2018). Effects of glutenin and gliadin modified by protein-glutaminase on pasting, rheological properties and microstructure of potato starch. *Food Chemistry, 253*, 148–155. https://doi.org/10.1016/j.foodchem.2018.01.155

Cui, M., Fang, L., Zhou, H., & Yang, H. (2014). Effects of amino acids on the physiochemical properties of potato starch. *Food Chemistry, 151*, 162–167. https://doi.org/10.1016/j.foodchem.2013.11.033

Farshi, P., Mirmohammadali, S. N., Rajpurohit, B., Smith, J. S., & Li, Y. (2024). Pea protein and starch: Functional properties and applications in edible films. *Journal of Agriculture and Food Research, 15*, Article 100927. https://doi.org/10.1016/j.jafr.2023.100927

Heyman, B., Depypere, F., Meeren, P. V. D., & Dewettinck, K. (2013). Processing of waxy starch/xanthan gum mixtures within the gelatinization temperature range. *Carbohydrate Polymers, 96*(2), 560–567. https://doi.org/10.1016/j.carbpol.2012.10.076

Hou, C., Zhao, X., Tian, M., Zhou, Y., Yang, R., Gu, Z., et al. (2020). Impact of water extractable arabinoxylan with different molecular weight on the gelatinization and retrogradation behavior of wheat starch. *Food Chemistry, 318*, Article 126477. https://doi.org/10.1016/j.foodchem.2020.126477

Hu, Y., He, C., Zhang, M., Zhang, L., Xiong, H., & Zhao, Q. (2020). Inhibition from whey protein hydrolysate on the retrogradation of gelatinized rice starch. *Food Hydrocolloids, 108*, Article 105840. https://doi.org/10.1016/j.foodhyd.2020.105840

Ji, X., Chen, J., Jin, X., Chen, J., Ding, Y., Shi, M., et al. (2023). Effect of inulin on thermal properties, pasting, rheology, and in vitro digestion of potato starch. *Starch - Stärke, 75*, Article 2200217. https://doi.org/10.1002/star.202200217

Kett, A. P., Chaurin, V., Fitzsimons, S. M., Morris, E. R., O'Mahony, J. A., & Fenelon, M. A. (2013). Influence of milk proteins on the pasting behaviour and microstructural characteristics of waxy maize starch. *Food Hydrocolloids, 30*(2), 661–671. https://doi.org/10.1016/j.foodhyd.2012.08.002

Kong, B., Niu, H., Sun, F., Han, J., & Liu, Q. (2016). Regulatory effect of porcine plasma protein hydrolysates on pasting and gelatinization action of corn starch. *International Journal of Biological Macromolecules, 82*, 637–644. https://doi.org/10.1016/j.ijbiomac.2015.10.026

Kuang, J., Huang, J., Ma, W., Min, C., Pu, H., & Xiong, Y. L. (2022). Influence of reconstituted gluten fractions on the short-term and long-term retrogradation of wheat starch. *Food Hydrocolloids, 130*, Article 107716. https://doi.org/10.1016/j.foodhyd.2022.107716

Kuang, J., Ma, W., Pu, H., Huang, J., & Xiong, Y. L. (2021). Control of wheat starch rheological properties and gel structure through modulating granule structure change by reconstituted gluten fractions. *International Journal of Biological Macromolecules, 193*, 1707–1715. https://doi.org/10.1016/j.ijbiomac.2021.11.008

Kuang, J., Yang, Q., Huang, J., Cao, Y., Pu, H., Ma, W., et al. (2022). Curdlan-induced rheological, thermal and structural property changes of wheat dough components during heat treatment. *Journal of Cereal Science, 107*, Article 103528. https://doi.org/10.1016/j.jcs.2022.103528

Kumar, L., Brennan, M., Brennan, C., & Zheng, H. (2022). Influence of whey protein isolate on pasting, thermal, and structural characteristics of oat starch. *Journal of Dairy Science, 105*, 56–71. https://doi.org/10.3168/jds.2021-20711

Lam, A. C. Y., Karaca, A. C., Tyler, R. T., & Nickerson, M. T. (2018). Pea protein isolates: Structure, extraction and functionality. *Food Reviews International, 34*(2), 126–147. https://doi.org/10.1080/87559129.2016.1242135

Liang, Y., Chen, Z., Liu, M., Qu, Z., Liu, H., Song, J., et al. (2022). Effect of curdlan on the aggregation behavior and structure of gluten in frozen-cooked noodles during frozen storage. *International Journal of Biological Macromolecules, 205*, 274–282. https://doi.org/10.1016/j.ijbiomac.2022.02.085

Lu, Z. X., He, J. F., Zhang, Y. C., & Bing, D. J. (2020). Composition, physicochemical properties of pea protein and its application in functional foods. *Critical Reviews in Food Science and Nutrition, 60*(15), 2593–2605. https://doi.org/10.1080/10408398.2019.1651248

Niu, L., Wu, L., & Xiao, J. (2017). Inhibition of gelatinized rice starch retrogradation by rice bran protein hydrolysates. *Carbohydrate Polymers, 175*, 311–317. https://doi.org/10.1016/j.carbpol.2017.07.070

Pang, Z., Bourouis, I., Sun, M., Cao, J., Liu, P., Sun, R., et al. (2022). Physicochemical properties and microstructural behaviors of rice starch/soy proteins mixtures at different proportions. *International Journal of Biological Macromolecules, 209*, 2061–2069. https://doi.org/10.1016/j.ijbiomac.2022.04.187

Qiu, C., Li, X., Ji, N., Qin, Y., Sun, Q., & Xiong, L. (2015). Rheological properties and microstructure characterization of normal and waxy corn starch dry heated with soy protein isolate. *Food Hydrocolloids, 48*, 1–7. https://doi.org/10.1016/j.foodhyd.2015.01.030

Qiu, S., Yadav, M. P., Chen, H., Liu, Y., Tatsumi, E., & Yin, L. (2015). Effects of corn fiber gum (CFG) on the pasting and thermal behaviors of maize starch. *Carbohydrate Polymers, 115*, 246–252. https://doi.org/10.1016/j.carbpol.2014.08.071

Qiu, S., Yadav, M. P., Liu, Y., Chen, H., Tatsumi, E., & Yin, L. (2016). Effects of corn fiber gum with different molecular weights on the gelatinization behaviors of corn and wheat starch. *Food Hydrocolloids, 53*, 180–186. https://doi.org/10.1016/j.foodhyd.2015.01.034

Ratnayakea, W. S., Hoovera, R., & Warkentin, T. (2002). Pea starch: Composition, structure and properties - a review. *Starch/Stärke, 54*, 217–234. https://doi.org/10.1002/1521-379X(200206)54:6<217::AID-STAR217>3.0.CO;2-R

Ribotta, P. D., Colombo, A., & Rosell, C. M. (2012). Enzymatic modifications of pea protein and its application in protein-cassava and corn starch gels. *Food Hydrocolloids, 27*(1), 185–190. https://doi.org/10.1016/j.foodhyd.2011.07.006

van der Sman, R. G. M. (2012). Soft matter approaches to food structuring. *Advances in Colloid and Interface Science, 176-177*, 18–30. https://doi.org/10.1016/j.cis.2012.04.002

Sun, Q., Sun, C., & Xiong, L. (2014). Functional and pasting properties of pea starch and peanut protein isolate blends. *Carbohydrate Polymers, 101*, 1134–1139. https://doi.org/10.1016/j.carbpol.2013.10.064

Tang, M. C., & Copeland, L. (2007). Investigation of starch retrogradation using atomic force microscopy. *Carbohydrate Polymers, 70*, 1–7. https://doi.org/10.1016/j.carbpol.2007.02.025

Wang, L., Ye, F., Li, S., Wei, F., Wang, Y., & Zhao, G. (2017). Effects of oat β-glucan incorporation on the gelatinization, flowability and moisture sorption of wheat flour. *Powder Technology, 315*, 430–437. https://doi.org/10.1016/j.powtec.2017.04.039

Wang, S., Zheng, M., Yu, J., Wang, S., & Copeland, L. (2017). Insights into the formation and structures of starch-protein-lipid complexes. *Journal of Agricultural and Food Chemistry, 65*(9), 1960–1966. https://doi.org/10.1021/acs.jafc.6b05772

Wu, C., Gong, X., Zhang, J., Zhang, C., Qian, J. Y., & Zhu, W. (2023). Effect of rice protein on the gelatinization and retrogradation properties of rice starch. *International Journal of Biological Macromolecules, 242*, Article 125061. https://doi.org/10.1016/j.ijbiomac.2023.125061

Wu, D. T., Li, W. X., Wan, J. J., Hu, Y. C., Gan, R. Y., & Zou, L. (2023). A comprehensive review of pea (Pisum sativum L.): Chemical composition, processing, health benefits, and food applications. *Foods, 12*, 2527. https://doi.org/10.3390/foods12132527

Xu, K., & Kuang, J. (2024a). Unraveling the mechanisms of pea protein isolate in modulating retrogradation behavior of pea starch. *Food Hydrocolloids, 156*, Article 110354. https://doi.org/10.1016/j.foodhyd.2024.110354

Xu, K., & Kuang, J. (2024b). Rheological, thermal, and structural properties of heat-induced gluten gel: Effects of starch with varying degrees of debranching. *International Journal of Biological Macromolecules, 272*, Article 132678. https://doi.org/10.1016/j.ijbiomac.2024.132678

Yang, C., Zhong, F., Goff, H. D., & Li, Y. (2019). Study on starch-protein interactions and their effects on physicochemical and digestible properties of the blends. *Food Chemistry, 280*, 51–58. https://doi.org/10.1016/j.foodchem.2018.12.028

Zhang, B., Qiao, D., Zhao, S., Lin, Q., Wang, J., & Xie, F. (2021). Starch-based food matrices containing protein: Recent understanding of morphology, structure, and properties. *Trends in Food Science & Technology, 114*, 212–231. https://doi.org/10.1016/j.tifs.2021.05.033

Zheng, M., Su, H., You, Q., Zeng, S., Zheng, B., Zhang, Y., et al. (2019). An insight into the retrogradation behaviors and molecular structures of lotus seed starch-hydrocolloid blends. *Food Chemistry, 295*, 548–555. https://doi.org/10.1016/j.foodchem.2019.05.166

Zhou, Y., Winkworth-Smith, C. G., Wang, Y., Liang, J., Foster, T. J., & Cheng, Y. (2014). Effect of a small amount of sodium carbonate on konjac glucomannan-induced changes in thermal behavior of wheat starch. *Carbohydrate Polymers, 114*, 357–364. https://doi.org/10.1016/j.carbpol.2014.08.033

Zhu, F., Bertoft, E., & Li, G. (2016). Morphological, thermal, and rheological properties of starches from maize mutants deficient in starch synthase III. *Journal of Agricultural and Food Chemistry, 64*(34), 6539–6545. https://doi.org/10.1021/acs.jafc.6b01265